

Impacts of the African Humid Period termination may have been delayed in the Atlantic Sahara

Juliana Nogueira^{1,2}, Heitor Evangelista², Abdelfettah Sifeddine³, Ahmed ElMouden⁴,
Lhoussaine Bouchaou^{4,5}, Mercedes Mendez-Millan³, Sandrine Caquineau³, Patricia
Piacsek⁶, Francisco Javier Briceño-Zuluaga⁷, Hugues Boucher³, Moussa Masrour⁴, Lucie
Juříčková⁸

¹ Faculty of Forestry and Wood Sciences, Czech University of Life Sciences Prague. Kamýcká 129. 165 00. Prague, Czech Republic

² LARAMG – Radioecology and Climate Change Laboratory, Department of Biophysics and Biometry, Rio de Janeiro State University. Rua São Francisco Xavier, 524. 20550-013. Rio de Janeiro, RJ, Brazil.

³IRD, Sorbonne Université, CNRS, MNHN, IPSL, LOCEAN, Bondy, France.

⁴ Laboratory of Applied Geology and Geo-Environment, Ibn Zohr University, Agadir, Morocco.

⁵ International Water Research Institute (IWRI), Mohammed VI Polytechnic University (UM6P), Ben Guerir, Morocco.

⁶ Centro de Geociencias, Universidad Nacional Autónoma de México (UNAM), Blvd. Juriquilla 3001, Campus UNAM 3001, 76230 Juriquilla, Querétaro, México.

⁷ Facultad de Ciencias Básicas - Universidad Militar Nueva Granada, Bogotá, Colombia.

⁸ Department of Zoology, Faculty of Science, Charles University, Viničná 7, CZ-128 44 Praha 2, Czech Republic.

Corresponding author: snogueira.j@gmail.com, Twitter: @PaleoJuh

This paper is a non-peer reviewed preprint submitted to EarthArXiv and will be submitted soon to Communications Earth & Environment

ABSTRACT

The paleoenvironmental changes recorded at the Khnifiss Lagoon, on the Saharan Atlantic coast, southern Morocco, during the last 3.5 kyrs BP puts another piece to the puzzle on the intricate relationship between North Atlantic climate patterns and climate variations in Northwest Africa. This study shed light on the hydroclimatic dynamics during a pivotal climatic period: the transition from the mid- to late Holocene and the termination of the African Humid Period. Our research unveils two key periods of salt marsh expansion at the Khnifiss Lagoon, approximately 3.5 and 2.7 kyrs BP when humidity conditions and increased marine influence were recorded. Those conditions paint a scenario of increased storminess and precipitation in NW Africa, compatible with a negative NAO-like climatic configuration. Our data revealed a synchronization between this scenario in NW Africa and cooling events in the North Atlantic during the transition from the mid-to-late Holocene, related to Rapid Climate Changes (RCCs) occurring between 3.5 and 2.5 kyrs BP, also known as the Bond event #2. These findings can potentially enhance climate prediction models, offering opportunities to better prepare for and adapt to the evolving climate patterns in the region. High-resolution paleoenvironmental records are still rare in Northwest Africa and are highly needed. The knowledge gained from these studies represents a critical step towards addressing the climate challenges in Northwest Africa and fortifying the region's resilience in the face of climate change.

Keywords: Africa; Coastal wetlands; Climate change; Holocene; African Humid Period; Paleolimnology; Sedimentology.

54 INTRODUCTION

55 Climate change and its impacts on the environment and societies represent one of the most
56 significant challenges of this century. Africa is one of the most climate-vulnerable continents
57 due to the combined effect of its significant exposure to climate change and its low
58 socioeconomic adaptive capacity ¹. In the last decade, the northwest coast of Morocco has
59 been hit by severe winter storms and occasional cyclones, causing extensive damage to the
60 environment and society ².

61 Situated along Africa's northern tectonic plates, Morocco faces various meteorological and
62 seismic threats, including earthquakes ³, tsunamis ⁴, landslides ⁵, inundations ⁶, marine
63 storms ², and the impacts of rising sea levels due to global climate change ⁷. Marine winter
64 storms cause intense flooding, beach erosion, and severe damage to roads and tourist
65 facilities ². Morocco boasts a coastal zone that stretches for over 3,500 kilometers along the
66 Atlantic Ocean and the Mediterranean Sea, encompassing a maritime area of approximately
67 1.2 million square kilometers and a fishing potential estimated by the FAO (United Nations
68 Food and Agriculture Organization) at nearly 1.5 million tons, renewable every year ⁸. The
69 fishing sector in Morocco is the third most significant contributor to the national economy,
70 following only agriculture and tourism. The Atlantic coast of Morocco is under many human
71 pressures, including urban expansion, pollution, and excessive exploitation of coastal
72 resources ⁹. Furthermore, high-energy marine events, such as marine storms, are increasing
73 the stress in the region, leading to short-term inundation of coastal lowlands, posing a threat
74 to people's safety and infrastructure ¹⁰.

75 Therefore, a better understanding of climate change's impact, such as increased storminess,
76 on Moroccan coastal environments and population is needed. However, information on
77 climate change in Northwest Africa, and especially in the Atlantic Sahara, remains scarce,
78 especially from the point of view of long records covering important periods in the Earth's
79 climate history ¹¹.

80 While the Holocene is generally regarded as a period of relative climatic stability, the
81 transition from the mid to late Holocene was marked by significant environmental changes
82 ¹²⁻¹⁴. This shift in Africa represented the transition from the “African Humid Period” during
83 the early Holocene to a drier late Holocene phase ¹⁵. Influenced by enhanced summer
84 insolation over North Africa and the consequent latitudinal displacement and contraction of
85 the Intertropical Convergence Zone (ITCZ), the W Africa monsoonal system underwent a
86 shift in its northward extent ¹⁵⁻¹⁹. The West African monsoonal system was pivotal in
87 governing moisture transport to Northwestern Africa, triggering substantial alterations in the
88 hydrological cycle and vegetation cover ^{18,20}. Both models ^{21,22} and proxy-based
89 reconstructions ^{15,16,23} suggest that this shift led to an amplification of the monsoonal climate
90 system and its northward reach due to feedback mechanisms involving vegetation, soil ²⁴
91 and extended water bodies ²⁵.

92 However, several questions surrounding the aridification patterns in Northwest Africa during
93 the mid to late Holocene persist. These inquiries revolve around three key aspects: first, the
94 exact timing of this transition ^{15,16,26,27}; second, whether this shift towards arid conditions
95 was generally abrupt ^{18,21,28-30}, and finally, the extent of the monsoonal influence reaching
96 northward ^{28,31,32}. Clarifying these questions is vital for gaining a more comprehensive
97 understanding of the hydroclimatic dynamics during this significant period in the Holocene
98 and the environmental feedback.

99 North Africa is a pivotal region for examining the intricate connections between low-latitude
100 African monsoon systems and large-scale millennial climate change ³³. The
101 paleoenvironmental reconstruction of coastal deposits provides valuable insights into
102 climate change and sea level changes caused by global to regional-scale exogenic processes
103 ³⁴. The primary obstacle when it comes to researching Holocene paleoenvironments in arid
104 regions lies in the somewhat limited preservation potential of sediments ³⁵. This limitation
105 poses a significant challenge to creating a comprehensive climatic change record. For this

106 reason, rare records are found within the region ^{11,18,36,37} and even fewer are located by the
107 coast ^{38,39}, which underscore the importance of our specific record in the northwestern
108 Sahara region.

109 In this study, we employ a multiproxy approach to document the paleoenvironmental
110 transformations that have taken place in the Khnifiss Lagoon, located in southern Morocco,
111 over the past 3.5 thousand years Before Present (kyrs BP). By reconstructing the
112 paleoenvironment at this unique site, situated on the Saharan Atlantic coast, we aim to shed
113 light on the hydroclimatic dynamics during a pivotal climatic period: the transition from the
114 mid to late Holocene and the termination of the African Humid Period. Furthermore, the
115 strategic latitudinal position of the Khnifiss Lagoon allows us to assess the interplay of
116 Northern Hemisphere climate patterns and the low-latitude African monsoon system on the
117 hydro-climate of northwest Africa and their variability in the past. Herein, the
118 paleoenvironmental reconstruction of a coastal lagoon in NW Africa recorded the impact of
119 increased storminess over the region and a relative delay in the drying tendency after the
120 mid Holocene, revealing an apparent synchronization between those events and the
121 occurrence of cooling events in the North Atlantic. Given the lack of studies in this
122 important climatic region, we expect that our results will contribute to understanding
123 hydroclimate variability in the transition from mid- to late Holocene and improve climate
124 prediction models that could enhance sustainable development and climate change
125 adaptation.

126

127 **METHODS**

128

129 **The Khnifiss Lagoon**

130 Situated along the southern Atlantic coast of Morocco, the Khnifiss Lagoon (28°02'54" N,
131 12°13'66" W) stretches for 20 km in length, covering an expansive surface area of 65 km²
132 (Fig. 1a). The Khnifiss Lagoon, including its salt flats, is the second most important wetland
133 in Morocco and the only tidal lagoon in the desert zone, providing shelter for a highly
134 diverse fauna, including wintering birds ⁴⁰. Data from the Ramsar sheet indicate that
135 Khnifiss Park is home to several vulnerable or threatened species at the national or
136 international level.

137 This coastal lagoon presents a small and shallow basin and rare freshwater input originating
138 from the temporary river (*Oued*) Aouedri. The lagoon is connected to the Atlantic Ocean by
139 a perennial inlet known as *Foum Agoutir*, leaving the lagoon subject to tidal influence ⁴¹.

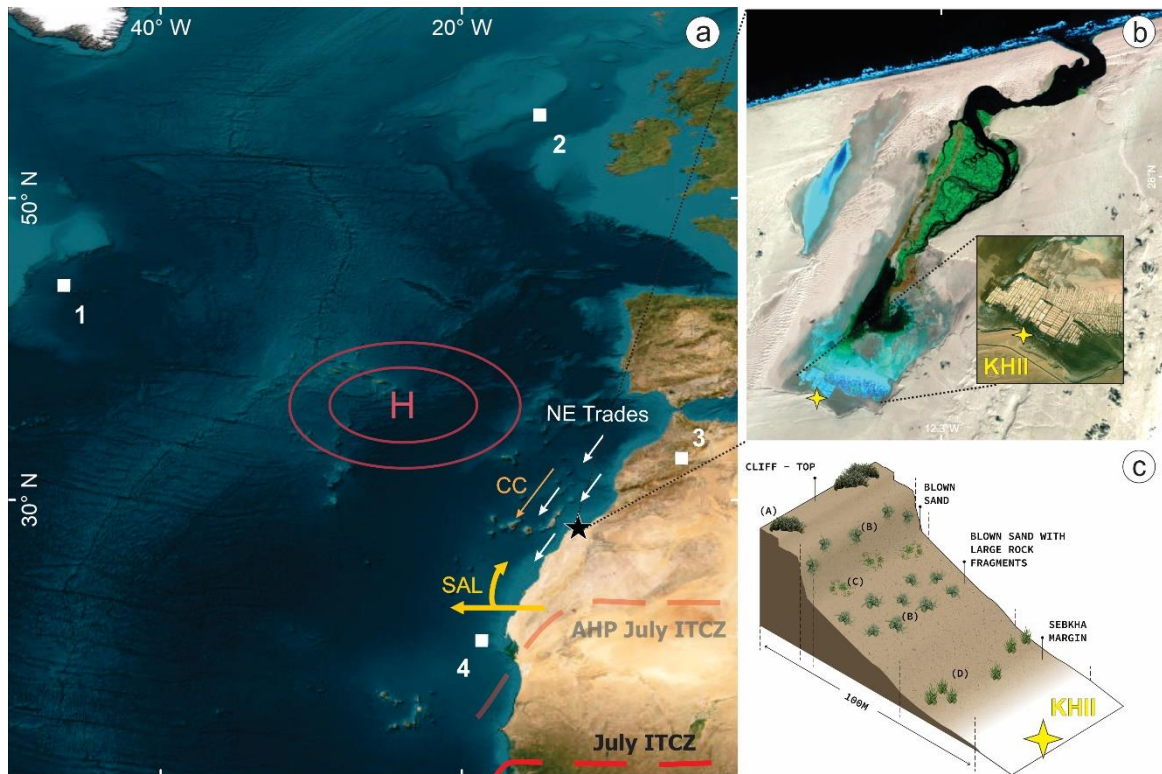
140 The lagoon features dendritic channels that fill progressively with the tides and narrow
141 upstream. The interconnected tidal channels are flanked by intertidal mudflats, a seagrass
142 bed (*Zoostera*), and an extensive tidal salt marsh, which only floods on the highest tides and
143 boasts a wide variety of vegetation. These salt marshes reveal a clear zoning pattern within
144 the tidal ecosystem, often attributed to the flora's resilience and adaptation to fluctuating
145 flood and salinity conditions.

146 The salt marsh extends upstream into the salt flat named *Sebkha Tazra*. However, due to its
147 distance from the inlet, most of *Sebkha Tazra* is unaffected by the tidal cycle and lacks
148 vegetation. During rare periods of rain or exceptionally high spring tides, *Sebkha Tazra* can
149 be briefly flooded ⁴². This extensive saltflat depression is enclosed by cliffs, and
150 groundwater lies close to its sandy floor. Due to this configuration, it is possible to observe a
151 thick salt crust formed after the evaporation of groundwater. In the northern and northeast
152 parts of *Sebkha Tazra*, we find transitional areas between salt marsh, desert reg, and salt flat,
153 where small communities of plants grow on small mounds of sand (Fig. 1c).

154 The Khnifiss Lagoon is under a hot desert climate (BWh), characteristic of dry, arid, low-
155 latitude deserts, according to the Köppen Climate Classification System. Previous works ⁴³⁻

156 ⁴⁵ describe southwestern Morocco under the influence of interannual to multidecadal
157 timescale climate changes and within the Saharan bioclimatic stage. Wind, humidity, and
158 precipitation in the region are associated with the North Atlantic Oscillation (NAO) phase
159 and the relative position of the Azores anticyclone, as it generates the trade winds that hit the
160 coast obliquely. The very same winds are associated with an important upwelling
161 phenomenon that occurs in the region of the Canary Current (CC), particularly near Cape
162 Ghir, as highlighted by previous research ⁴⁶ (Fig. 1a). A speleothem from southwestern
163 Morocco reveals a millennial long influence of both the NAO and the Atlantic Multidecadal
164 Oscillation (AMO) in the region ⁴⁴.

165 Previous research in the Khnifiss Lagoon suggests that, in the last century, the coast was
166 directly affected by NAO oscillations and sea level changes ⁴⁵. A combined approach with
167 remote sensing data and geochemical analysis reveals the sensitivity of the Khnifiss Lagoon
168 to large-scale climatic processes, such as NAO. During its positive phase, a strong east-to-
169 west wind leads to a widening of the inlet, which, in turn, affects the hydrodynamics and
170 biogeochemical cycles of the lagoon ⁴⁵. Previous studies indicate that the expansion of the
171 Khnifiss Lagoon and surrounding areas is governed by the inlet's dynamic, the sea level of
172 Morocco, and changes in the hydrological condition ^{45,47}. Therefore, our record has the
173 potential to improve further our knowledge of the climatic mechanisms and dynamics
174 influencing NW Africa environments during the last ~3.5 kyrs BP.



175 **Figure 1** – Geographical, climatic and ecological set of the Khnifiss Lagoon (black star). (a) Climatic
 176 mechanisms acting over south Morocco: CC (Canaries Current); SAL (Saharan Air Layer); latitudinal position
 177 of the Intertropical Convergence Zone (ITCZ) during winter in the present day (red dashed line) and in the
 178 African Humid Period (AHP; faded red dashed line); latitudinal position of the Azores High Pressure Zone (red
 179 H); (1) and (2) correspond to the marine cores presented by Bond et al.^{48,49} (MC52 + VM29191 and MC21 +
 180 GGC22), (3) Pollen reconstruction for the Atlas Mountain based on data from the sediment core at Lake
 181 Tigalmamine⁵⁰ (4) NW Africa Humidity Index marine sediment core GeoB7920²⁹. (b) The Khnifiss Lagoon
 182 remote sense image in the composition 543 where the vegetation (green), water (black) and salt flat (*sebkha*;
 183 blue) and the position of the KHII sediment core (yellow star) are highlighted. (c) vegetation distribution
 184 profile around the coring location.

185

186 **Sediment core**

187 To deepen our understanding of the region’s paleoclimatic dynamics and the changes in its
 188 paleoenvironment, we manually collected a sediment core from the innermost area of
 189 Sebkha Tazra in the Khnifiss Lagoon (KHII: 27°54 ‘55.1’ N, 12°22’04.4” W) (Fig. 1b).

190 Before opening, the sediment core was x-rayed using a Siemens 500 ma Polymat S Plus X-
 191 ray equipment operating at 85 kVp, 124 mA, 200 mAs. The gray scale of the image was
 192 generated using the software ImageJ. The sediment core was opened in half with a
 193 subsequent description of the most prominent visible features and the color following the
 194 Munsell chart. Subsequently, an X-ray fluorescence (XRF) analysis was performed using an

195 ARTAX Bruker AXS XRF spectrometer, operating at 25 kV and 500 mA, to obtain the
196 elementary mapping of the sample surface along the sediment core. The sediment core was
197 then sliced into 1-cm subsamples, and visible shells and other mineral specimens were
198 separated for further analysis.

199 The KHII sediment core was dated at the LMC14 Artemis Laboratory in Saclay, France,
200 according to the following methodology. Samples were treated in an excess of 0.5N
201 hydrochloric acid for several hours at 80°C to eliminate carbonates, then rinsed with
202 ultrapure water until neutral pH. Different quantities, depending on the % Total Organic
203 Carbon (TOC) of the samples, were taken to obtain, after combustion, a volume of CO₂
204 containing about 1 mg of carbon. The sample was burned in the presence of about 500 mg of
205 copper oxide and a silver wire for 5 hours at 835°C. The CO₂ was then reduced by hydrogen
206 in the presence of iron powder at 600°C. The mass of iron is equal to 3 times the mass of
207 carbon, with a minimum value of 1.5 mg and a maximum value of 4 mg. The carbon
208 deposited on the iron powder and the assembly was pressed into a support for measurement
209 by Accelerator Mass Spectrometry (AMS). The ¹⁴C activity of the sample was calculated by
210 comparing the sequentially measured intensities of the ¹⁴C, ¹³C, and ¹²C beams of each
211 sample with those of CO₂ standards prepared from the reference oxalic acid HOxII and
212 expressed in pMC (percent Modern Carbon) normalized to a deltaC13 of -25 per thousand.
213 Radiocarbon ages were calculated according to Mook and van der Plicht (1999) in
214 correcting the fractionation with the deltaC13 calculated from the ¹³C/¹²C ratio measured on
215 ARTEMIS. The deltaC13 used included fractionation during both sample preparation and
216 the SMA measurement. Measurement uncertainty accounted for both statistical error and
217 measurement variability for the sample and the subtracted blank.

218 To determine the origin of sedimentary organic matter, elemental and isotopic carbon
219 concentrations were analyzed in samples after acid attack (HCl 3%) to remove the carbonate
220 fraction. δ¹³C and organic carbon determination were performed in a FlashHT 2000

221 elemental analyzer coupled with a Delta V Advantage mass spectrometer from Thermo
222 Fisher Scientific with a precision of 0.05 per mil for $\delta^{13}\text{C}$ and 0.05% for organic carbon. The
223 $\delta^{13}\text{C}$ is expressed in per mil (‰) against the international standard VPDB (Vienna Pee Dee
224 Belemnite).

225 To determine the composition of three mineral specimens recovered from the sediment core,
226 finely crushed sub-samples were deposited on a flat silicon (Si) monocrystal support. X-ray
227 diffraction (XRD) patterns of the samples were recorded on a Panalytical X'Pert Powder
228 diffractometer equipped with a PIXcel detector (255 active channels) and Cu anticathode
229 operating at 40 kV and 40 mA. The diffractograms were measured in the 3° - 70° 2θ range
230 with a step size. Mineral identification was performed using Highscore 3.0 software and two
231 databases: ICSD (Inorganic Crystal Structure Database) and COD (Crystallography Open
232 Database).

233 Preserved specimens of mollusk shells, preferably whole, were separated for identification
234 during core subsampling. The samples were subjected to an ultrasonic bath for two rounds
235 of 1 minute using ultrapure water to remove the deposited material. Specimens were
236 identified by specialists at the Department of Zoology, Charles University (Czech Republic)
237 and at the Laboratory of Applied Geology and Geo-Environment, Ibn Zohr University
238 (Morocco), taking into account the species distribution at the Khnifiss Lagoon and later
239 photographed.

240 A principal component analysis (PCA) was performed using Statistica software by StatSoft
241 to support multi-proxy interpretation and discussion.

242

243

244

245 **RESULTS AND DISCUSSION**

246 **The Khnifiss Lagoon paleoenvironment in the last 3.5 kyr**

247 The 207 cm sediment core has shown clear zonation that reflects the paleoenvironmental
248 changes that occurred in the Khnifiss Lagoon (Fig. 2). To understand the timing of those
249 changes, we focused on the portion between 155 and 227 cm of depth and dated four key
250 positioned samples (160-161: 2769 ± 27 cal yrs BP, 185-186: 6587 ± 56 cal yrs BP, 202-203:
251 3442 ± 35 cal yrs BP and 218-219: 3428 ± 29 cal yrs BP). Dating of coastal lagoons inserted
252 in semi-/arid areas is challenging and outliers, as the one in sample 185-186, can be common
253 ^{10,52} mainly due to remobilization or periods of intense desiccation cycles. Although, we
254 acknowledge the limitations derived from the reduced number of ¹⁴C samples, we are
255 convinced that this chronology should not limit the analysis of the overall trend recorded
256 over the past ~3.5 kyrs and described as it follows.

257

258

259

260

261

262

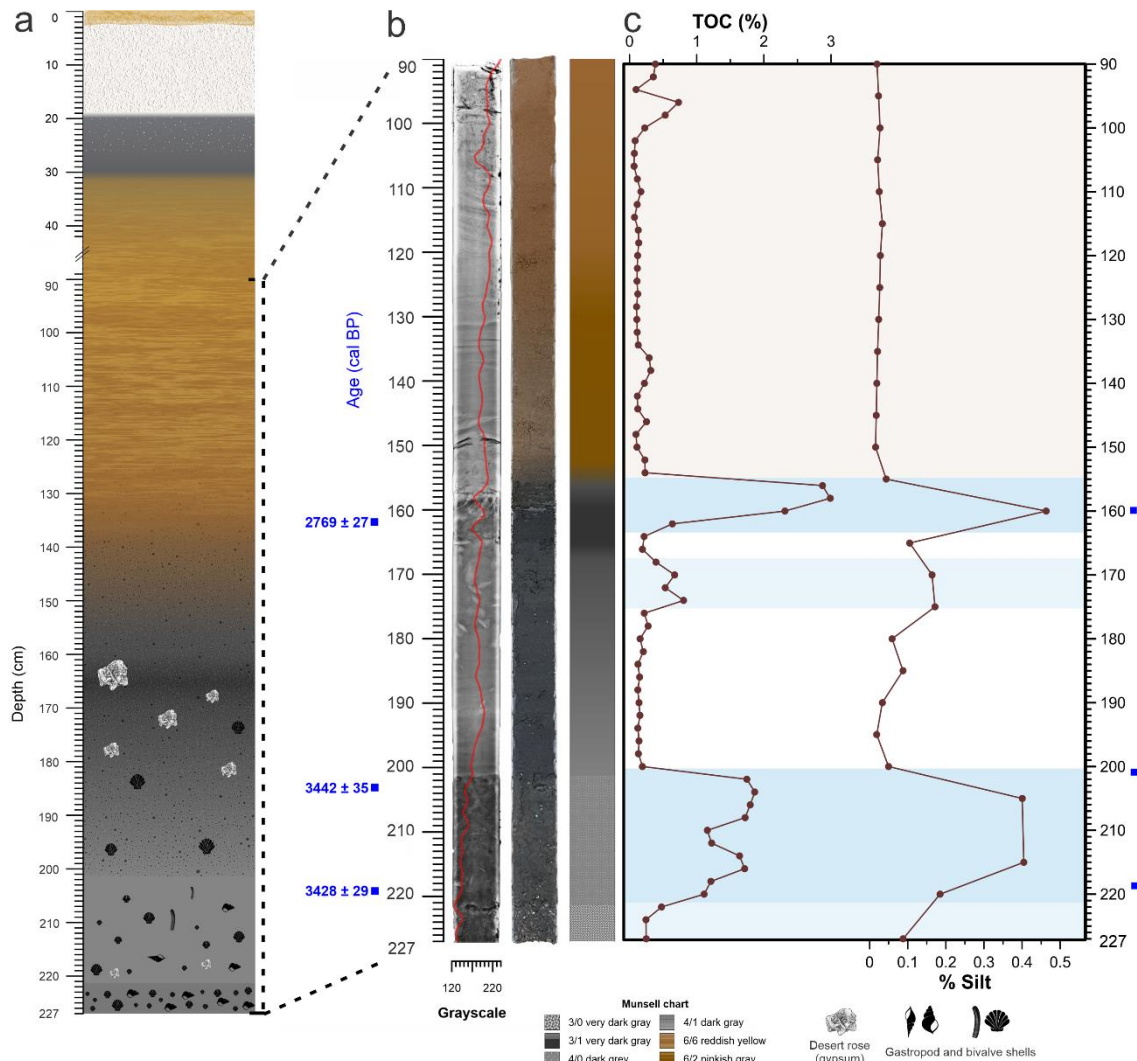
263

264

265

266

267



268 **Figure 2** – KHII sediment core profile (a), x-ray (b), photography, and (c) TOC and silt variation. Blue shading
 269 represents periods of higher humidity, while orange shading refers to dry periods.

270

271 The first phase, corresponding to the period before 3428 ± 29 cal yrs BP (221 – 227 cm),
 272 shows a continuous increase of COT ($\mu = 0.97\%$), C/N, and silt, followed by a decrease in
 273 salinity (Fig. 3), as indicated by the Sr/Ca ratio⁴⁵. In a previous study, the isotope and
 274 elemental signatures of vegetation within Khnifiss Park were reported (Nogueira et al.,
 275 2022). This information served as the basis for interpreting the C/N vs. $\delta^{13}\text{C}$, suggesting a
 276 combined contribution of submerged vegetation and phytoplankton. The abundant presence
 277 of mollusk shells (*Cerastoderma edule*, *Dosinea exoleta*, *Giberulla miliaria*,
 278 *Calliostomatidae*, and *Nasaridae*) suggests a perennial presence of water during this period.
 279 The mentioned species inhabit intertidal muddy sand flats and are also typically associated

280 with *Zoostera* grass beds. Granulometry during this period indicated a muddy sand substrate
281 characterized by poorly sorted grains that varied in the size of medium sand and very coarse
282 silt. The combined interpretation of the proxies points to an environment with a perennial
283 presence of water and a gradual development of pioneer marsh vegetation ⁴⁵. Therefore, a
284 progressive increase in water levels, the related drop in salinity, and the predominance of
285 marine dinoflagellate cysts may indicate a greater marine influence during this period.

286 The second phase, centered around 3435 ± 32 cal yrs BP (201 – 221 cm), shows an increase
287 in TOC ($\mu = 1.52\%$) content and a displacement towards higher C/N values. The C/N vs.
288 $\delta^{13}\text{C}$ diagram points to an increased contribution of eventually submerged salt marsh
289 vegetation. At the same time, the amount of titanium, here used as a proxy for silt/clay
290 minerals ⁵³, increases, reflecting changes in the soil possibly related to marsh development.
291 The large drop in salinity and the continuous presence of marine dinoflagellate cysts and
292 *Chenopodiaceae* pollen corroborate the interpretation of a well-developed salt marsh with
293 high marine influence, as also described for the lagoon Moulay-Boulsalham in north
294 Morocco ⁵⁴. Although less abundant, mollusks such as *Cerastoderma edule*, *Odostomia sp.*,
295 *Solen sp.*, *Turitella sp.*, Nassaridae, Mathildidae are still present and are known to typically
296 inhabit *Zostera* seagrass and intertidal zones, possibly indicating the low tide mark. In
297 general, during phase II there is an established salt marsh, with constant presence of water,
298 increased marine influence, and high sedimentation rate (20 cm deposited around 3435 ± 32
299 cal yrs BP).

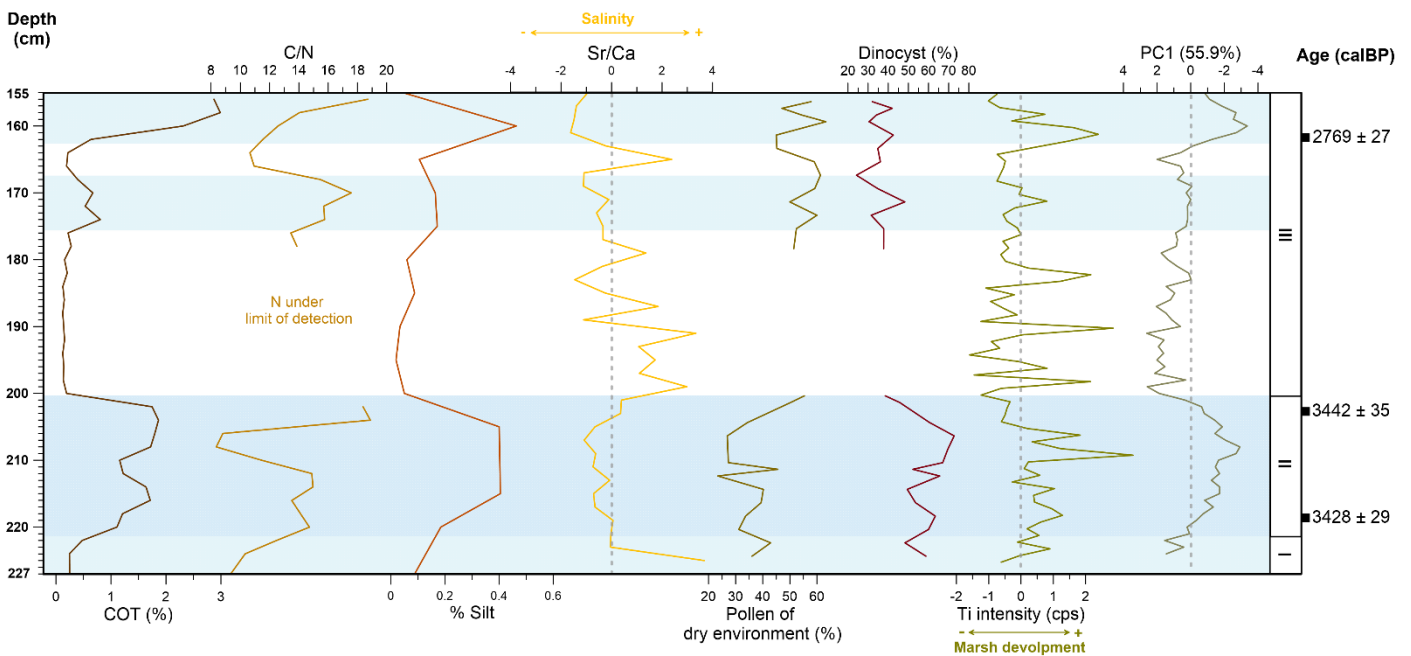
300 The third phase, which occurred between 3435 ± 32 cal yrs BP and $\sim 2769 \pm 27$ cal yrs BP
301 (155 – 201 cm), records a dramatic environmental change. At the beginning of this phase,
302 between 175 and 201 cm, a very low TOC ($\mu = 0.17\%$) is found, and nitrogen values are
303 lower than the detection limit. This could indicate a possible organic matter decomposition,
304 denitrification, and volatilization of nitrogen compounds as the lagoon, at this point, dries
305 out. Furthermore, no dinoflagellate cysts or pollens were found during this period. The grain

306 size analysis shows moderately well and moderately sorted fine and medium sand grains,
307 generally associated with a selective sedimentation agent, such as the wind. Indeed, the x-
308 ray image (Fig. 2b) reveals a lamination pattern of deposition during this phase. Aeolian-
309 deposited sand typically displays wind-ripple laminations characterized by planar-parallel
310 and undulatory layers and fine to medium grains⁵⁵. Thus, a predominant aeolian influence
311 was occurring at the distal point of the Khnifiss Lagoon during the beginning of the third
312 phase. The water would still arrive at this point, probably per percolation initially, and later,
313 towards the end of this phase, forming a shallow water column accompanied by a decrease
314 in salinity. Between 165 and 175 cm, it is possible to observe a significant number of
315 crystalline structures identified by DRX analysis as gypsum rosettes. The presence of these
316 minerals of evaporites is associated with rapid fluctuations of water in an arid environment
317 rich in CaSO₄, especially in shallow-water saline lakes and lagoons that go through repeated
318 cycles of dissection⁵⁶. During this phase, it is possible to observe two brief increases in
319 TOC: the first one centered around 173 cm and the second and highest one centered around
320 160 cm (i.e., around 2769 ±27 cal yrs BP) that are both accompanied by a drop in salinity.
321 These could indicate a brief return of marine influence, allowing a discreet salt marsh to
322 develop in the distal part of the lagoon. This interpretation is corroborated by the low
323 presence of dinocysts and the increased presence of pollens of dry environments. This phase
324 is abruptly interrupted in 2769 ± 27 cal yrs BP (30 – 155 cm) by dry conditions indicated by
325 a laminated reddish yellow (6/6) sand associated with aeolian transportation and deposition.
326 The well-sorted and rounded sand-grain population shows that the source of aeolian sand
327 may have become dominated by coastal dunes.

328 A thick layer of approximately 16 cm of salt covered by loose sand tops the laminated sand
329 (Figure 2a). The salt crust is then followed by a gray sticky silt layer (4/0 dark gray) of about
330 10 cm. This layer's average organic carbon content is 0.51%, except for the most recent
331 layer, which presents 2.17%. The presence of crust and grey silt is due to variations in

332 groundwater level, which is linked to variations in local rainfall, sea level, and hydrological
 333 changes⁵⁷.

334 In summary, in contrast to the established *Sebkha* seen today, a developed salt marsh was
 335 present $\sim 3435 \pm 32$ cal yrs BP and $\sim 2769 \pm 27$ cal yrs BP, indicating an advance in the
 336 marine influence even in the most continental portions of the lagoon. The current arid
 337 condition, therefore, was only completely established after 2769 ± 27 cal yrs BP. These
 338 significant shifts in environmental parameters highlight the dynamic nature of the region's
 339 ecosystem during these particular timeframes.



340 **Figure 3** – KHII's main proxies' profile and phases.

341

342 **Holocene Climate Variability and Coastal Responses in Northwest Africa**

343 In the present days, during the boreal winter season, the characteristics of storms, including
 344 their location, intensity, and frequency in the North Atlantic, are predominantly influenced
 345 by the dynamics of the jet stream and the atmospheric pressure systems within the region.
 346 This relationship is elucidated by the NAO index, with anomalies correlated to fluctuations
 347 in solar activity, notably in ultraviolet radiation⁵⁸. In the positive phase of the NAO,

348 intensified westerly winds push the storm track northward, directing it towards northern
349 Europe. Consequently, this region witnesses warmer and wetter conditions, while northern
350 Africa and southern Europe face drier-than-normal weather. Conversely, during the negative
351 phase, the storm tracks shift southward, resulting in increased precipitation in the western
352 Mediterranean and northern Africa and causing northern Europe to experience colder and
353 drier conditions than usual ^{59–61}.

354 Throughout the Holocene, both models and paleoclimate reconstructions have indicated that
355 orbital changes led to a progressively steeper temperature gradient and an overall northward
356 shift in the storm track towards the present days ^{60–64}. In the late Holocene, the northern
357 hemisphere witnessed recurring cooling events, as documented by Bond et al.⁶⁵. These
358 events, potentially linked to reduced solar irradiance, may have given rise to a scenario
359 reminiscent of a negative phase of the NAO. This climatic pattern, a consequence of the
360 interplay of atmosphere-ocean dynamics, resulted in increased precipitation and storm
361 activity across southern Europe and North Africa ⁶⁶. Data from a marine core retrieved off
362 the coast of western Africa (at 20° N) indicates that the Holocene climatic cycles closely
363 paralleled synchronous changes in Sea Surface Temperature (SST), emphasizing a strong in-
364 phase relationship between high- and low-latitude climates ¹⁵.

365 Our sediment core has documented two periods of salt marsh expansion in the most inland
366 portions of the Khnifiss Lagoon in 3.5 kyrs BP (event 1 = E1) and 2.7 kyrs BP (event 2 =
367 E2). Coastal wetlands in arid regions can respond to changes in the i) relative sea level; ii)
368 fluvial apport variation; iii) precipitation amount; iii) wind structure linked to the tidal inlet
369 dynamics; and iv) extreme events such as tsunamis and storms ^{45,67–70}. At the ebb-dominated
370 Khnifiss Lagoon, previous studies indicated that when storm surges are directed to the
371 continent, increased wave energy causes an enhanced hydraulic slope in the flooding tide
372 within the inlet channel, leading to a net landward movement of sediment and water. This
373 process culminates in the upbuilding of the flood tidal delta – with the deposition of higher

374 grain size – and in the washover of smaller grain size sediments on the salt marsh, allowing
375 its development and expansion ^{45,47,69,71}. A comprehensive analysis, incorporating both
376 remote sensing data and geochemical assessments, has provided a detailed account of the
377 dynamics within the Khnifiss Lagoon over the past century. This investigation has suggested
378 varying degrees of sensitivity to climatic events depending on the proximity to the lagoon's
379 inlet. Notably, the more inland regions of the lagoon appear to be impacted solely by
380 significant climatic events ⁴⁵.

381 To comprehend the dynamics behind progradation events E1 and E2, we conducted a
382 Principal Components Analysis (PCA) using data on TOC content, Sr/Ca ratio, silt content,
383 and Ti from KHII. Notably, the first principal component accounted for a significant 56% of
384 the explained variance, as shown in Figure 5a, and revealed a distinct pattern characterized
385 by alternating phases of decrease and increase, which decreases were linked to salt marsh
386 accretion. These data are in agreement with different paleoenvironmental studies carried out
387 on the Moroccan Atlantic coast (Fig. 5b) that show high-energy-deposited-sediments
388 occurring at the same time as E1 and E2, suggesting a regional forcing causing these marine
389 transgressions. These on-shore deposits were reported in the form of fine sediments layers at
390 the estuaries of Tahaddart (35.5° N) ^{10,72} and Loukkos (35.15° N) ⁴ and at the Moulay-
391 Bousalham (34°N) and Oualidia (32°N) lagoons ^{38,39,54}, and marine gastropods shells
392 deposited at Moulay Douraine (31° N) ⁷³. Biogeographic evidence from the NW African
393 coast (28 – 19° N) suggests a transgression event taking place around 3.5 kyrs BP ⁷⁴, also
394 recorded by wetlands on the Atlantic coast of Spain in addition to another one around 2.8
395 kyrs BP ⁷⁵⁻⁷⁷. Changes in Holocene vegetation in France and southwest Spain indicate a
396 humid period between 3.4 and 2.8 kyrs BP, with two arid phases (4.3 – 3.4 kyrs BP and 2.8 –
397 1.7 kyrs BP) flanking it ⁷⁸ (Jalut et al. 2000). Along the Portuguese coast, a humid period
398 occurred around 3 kyrs BP, interrupting the drier conditions that preceded and followed it ⁷⁹.
399 Flood frequency records from northeastern Morocco also point to increased precipitation

400 between 3.2 and 2.7 kyrs BP⁸⁰. In the western Mediterranean, increased precipitation
401 recorded around 3.3 and 2.7 kyrs BP⁶⁶ coincided with low NAO stages⁸¹. Both simulations
402²⁵ and paleo records^{18,28,29,32,52,82–84} indicate humid conditions in the northern Africa around
403 3 kyrs. On a millennial timescale, coastal areas' sediments can become more or less likely to
404 record overwash deposition according to variations of relative sea level, inlet(s) position and
405 size, and sediment supply changes^{10,85,86}. This can lead to variations in the record of events'
406 frequency and intensity in the sediments, resulting in potential delays or omissions when
407 comparing these events across different environments. Nevertheless, the sediment records
408 along the Morocco, Iberian Peninsula, and the Mediterranean point to high-energy events
409 and humid conditions around 3.5 kyrs and 2.8 kyrs BP, impacting as south as 27° N. For the
410 Khnifiss Lagoon, the E2 relative lower sedimentation, when compared to E1, and the
411 abundance of gypsum rosettes during this period are climatically influenced and are a
412 consequence of the rising aridity trend observed in Morocco⁸⁷ (Fig. 5c) and NW Africa in
413 general²⁹ (Fig. 5d) that may have limited the saltmarsh accretion. Peak synchronism among
414 the Khnifiss Lagoon and other proxy records, as evident in Figure 5, indicates an influence
415 of storm surges that probably caused the inlet opening and widening and water to arrive
416 even in the most distant parts of the lagoon. In combination with a more humid climate, the
417 salt marsh thrived in this portion of the lagoon during these events; however, once drier
418 conditions settled in, the marsh gave way to a salt flat, present until these days.

419 Currently, the climate in our study region is dominated by the baroclinic variation over the
420 North Atlantic⁸⁸, and therefore, we hypothesize that our record can be compared to proxies
421 from higher latitudes in the northern hemisphere. Between 3.5 kyrs BP and 2.6 kyrs BP,
422 proxy records point to low temperatures in the Northern Hemisphere, as suggested by the
423 stacked record of Ice-Rafted Debris (IRD) reconstructed in the North Atlantic (Bond #2)¹⁴.

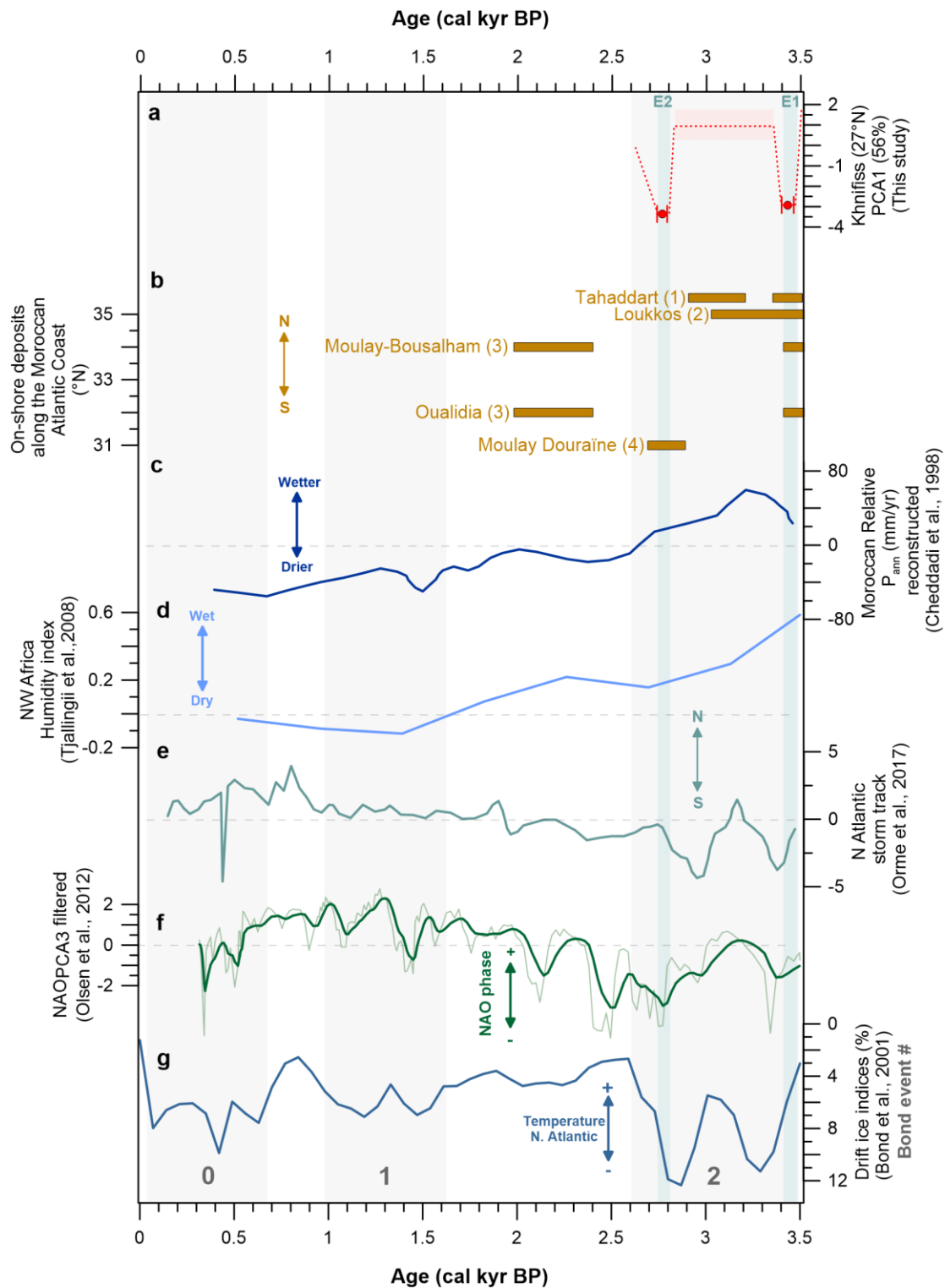
424 During the late Holocene, the cooling observed in the North Atlantic region may be
425 attributed to atmospheric-ocean dynamics, including changes in the strength of sub-tropical

426 gyres, as previously explained. This cooling increased precipitation over Northwestern
427 Africa and the Mediterranean, causing a southward shift in the storm tracks. These changes
428 are reflected in the North Atlantic storm index (Fig. 5e; ⁶⁴. This climatic scenario is
429 comparable with the present NAO negative phase ⁸⁹ and is evident in the reconstructed
430 Holocene NAO index⁸¹ (Fig. 5f) and pointed out previously⁸². When reviewing paleoclimate
431 records from diverse global regions, researchers have pinpointed up to six noteworthy
432 periods of rapid climate change (RCC) within the Holocene. A distinct cooling trend in polar
433 regions marked these RCC events. Among these, one particularly significant RCC event
434 unfolded between 3.5 and 2.5 kyrs BP ^{12,14} that may have been linked with the negative
435 NAO-like scenarios that impacted northwest Africa.

436 The termination of the African Humid Period (AHP) has been the subject of debate within
437 the scientific community, with most studies convergent on an overall abrupt climatic change
438 occurring at ~5.5 kyrs BP ^{15,18,90,91}. However, few other studies favor a more gradual
439 transition ^{21,28,29}. The Khnifiss Lagoon, located at 27°N, currently has a climate dominated
440 by the North Atlantic climate system ⁸⁸. However, during the Holocene, this latitude
441 represented the boundary between a dominance by this system at north and a monsoonal
442 climate system dominance at south ¹⁸. In the transition from mid- to late Holocene, this
443 region was under the influence of the northernmost expansion of the West African Summer
444 Monsoon (WASM) ^{11,28,31,32,36,83}. Therefore, the Khnifiss Lagoon's core, with its sensitivity
445 to the interplay of these two climatic systems, supports the idea of a gradual climate
446 transition in Northwest Africa's coastal regions and records humid conditions until ca 2.7
447 kyrs BP. This observation agrees with other studies that suggest that a humid period can be
448 clearly recognized from about 5 kyrs BP to 3 kyrs BP in North Africa ⁹² and until 2 kyrs BP
449 in south Morocco ⁹³. Hence, we claim that the proposed prolongation of wetter conditions in
450 the Atlantic Sahara was a consequence of the combination of i) RCC events characterized by
451 polar cooling that may have caused an NAO-like scenario that triggered the southward

452 migration and weakening of the Azores High and storminess over north Africa and ii) a
453 northward expansion of the West African Summer Monsoon (WASM). These conditions
454 sustain the concept of a possible teleconnection between hydrological conditions over
455 Northwest Africa and the North Atlantic climatic variability. On a smaller scale, our work, in
456 conjunction with Nogueira et al. ⁴⁵, highlights the resilience of coastal wetlands to climate
457 fluctuations. It underscores the significant influence of humidity conditions, particularly in
458 arid regions, on salt marsh accretion and inland expansion.

459 Anticipated global warming may reduce the temperature gradient in mid- to high latitudes,
460 causing winter storm tracks to shift southward and increasing the frequency of storms along
461 Morocco's Atlantic coast ⁶⁴. Enhancing our knowledge of the environmental feedback to
462 these changes is crucial in minimizing uncertainties associated with such shifts, which is
463 essential for effective climate adaptation strategies.



464 **Figure 4** – (a) Khnifiss first principal component (PCA1, 56%) compared to (b) other on-shore deposits along
 465 the Moroccan Atlantic coast at: (1) Tahaddart estuary¹⁰, (2) Loukkos estuary⁴, (3) Moulay-Bousalham and
 466 Oualidia coastal lagoons³⁹ and (4) Moulay Douraine⁹⁴; (c) Moroccan relative precipitation reconstruction
 467 based on pollen records⁵⁰; (d) NW Africa Humidity index²⁹; (e) North Atlantic storm track reconstruction⁶⁴;
 468 (f) North Atlantic Oscillation (NAO) reconstruction⁸¹ and (g) North Atlantic drift ice indices⁴⁸. Vertical gray
 469 bars and numbers represent the different Bond events while green vertical bars mark the timing of high energy
 470 events (Event 1: E1, Event 2: E2) recorded at the Khnifiss Lagoon.

471

472

473 CONCLUSION

474 The challenges posed by climate change in Morocco and Northwest Africa are significant
475 and multifaceted. The region grapples with environmental and societal threats like storms,
476 earthquakes, and rising sea levels, all exacerbated by urbanization and resource exploitation.

477 The research conducted in the Khnifiss Lagoon serves as a valuable window into the
478 transition from the mid to late Holocene, shedding light on the intricate relationship between
479 climate patterns in the North Atlantic and the climate in NW Africa.

480 The paleoenvironmental reconstruction in the Khnifiss Lagoon has revealed a
481 synchronization between increased storminess and delayed aridification in NW Africa and
482 cooling events in the North Atlantic during the mid- to late Holocene transition. As
483 previously suggested by other researchers, a negative NAO-like scenario could be
484 responsible for such circumstances in south Morocco. At the same time, these conditions
485 must have delayed the aridification trend in the north Saharan coastal environments, which
486 only started after about 2.7 kyrs BP. This suggests that the African Humid Period
487 termination, usually regarded as ca 5.5 kyrs BP, must have happened at different times
488 across North Africa due to environmental specificities. More research on the exact time and
489 nature of these changes, extending the knowledge further back in the past with high
490 resolution archives is needed to understand the extension of the impacts and the climatic
491 feedback between NW Africa and conditions in the North Atlantic.

492 The emphasis on understanding the dynamic interplay between climate fluctuations and
493 coastal environments highlights the resilience and adaptability of these regions. With the
494 specter of global warming on the horizon, research focusing on predicting possible changes
495 in storm patterns along Morocco's Atlantic coast is necessary. These findings can potentially
496 enhance climate prediction models, offering opportunities to better prepare for and adapt to
497 the evolving climate patterns in the region. Overall, the knowledge gained from these studies

498 represents a critical step towards addressing the climate challenges in Northwest Africa and
499 fortifying the region's resilience in the face of climate change.

500

501 REFERENCES

- 502 1. Niang, I. *et al.* Africa. in *Climate Change 2014: Impacts, Adaptation and Vulnerability - Contributions*
503 *of the Working Group II to the Fifth Assessment Report of the Intergovernmental Panel on Climate*
504 *Change*. 1199–1265 (Cambridge University Press, 2014).
- 505 2. Mhammdi, N. *et al.* Marine storms along the Moroccan Atlantic coast: An underrated natural hazard?
506 *J. African Earth Sci.* **163**, 103730 (2020).
- 507 3. Cherkaoui, T. & El Hassani, A. Seismicity and Seismic Hazard in Morocco 1901-2010. *Bull. l'Institut*
508 *Sci.* **34**, 45–55 (2012).
- 509 4. Mhammdi, N. *et al.* Sedimentary evidence of palaeo-tsunami deposits along the Loukkos estuary
510 (Moroccan Atlantic Coast). *Journal Tsunami Soc. Int.* **34**, 83–100 (2015).
- 511 5. Harmouzi, H. *et al.* Landslide susceptibility mapping of the Mediterranean coastal zone of Morocco
512 between Oued Laou and El Jebha using artificial neural networks (ANN). *Arab. J. Geosci.* **12**, 696
513 (2019).
- 514 6. *Wadi Flash Floods*. (Springer Singapore, 2022). doi:10.1007/978-981-16-2904-4.
- 515 7. Satta, A., Snoussi, M., Puddu, M., Flayou, L. & Hout, R. An index-based method to assess risks of
516 climate-related hazards in coastal zones: The case of Tetouan. *Estuar. Coast. Shelf Sci.* **175**, 93–105
517 (2016).
- 518 8. Royaume du Maroc. *Portrait de secteur de pêche maritime au Maroc*. (2015).
- 519 9. Snoussi, M., Khouakhi, A. & Niang-diop, I. Geomorphology Impacts of sea-level rise on the Moroccan
520 coastal zone : Quantifying coastal erosion and flooding in the Tangier Bay. **107**, 32–40 (2009).
- 521 10. Khalfaoui, O., Dezileau, L., Degeai, J. P. & Snoussi, M. A late Holocene record of marine high-energy
522 events along the Atlantic coast of Morocco: new evidences from the Tahaddart estuary.
523 *Geoenvironmental Disasters* **7**, (2020).

- 524 11. Ait Brahim, Y., Bouchaou, L. & Wanaim, A. Speleothem-based paleoclimate research in South
525 Morocco: Interest and perspectives. *Front. Sci. Eng.* **11**, 9–16 (2021).
- 526 12. Mayewski, P. a. *et al.* Holocene climate variability. *Quat. Res.* **62**, 243–255 (2004).
- 527 13. Haug, G. H. Southward Migration of the Intertropical Convergence Zone Through the Holocene.
528 *Science (80-.)*. **293**, 1304–1308 (2001).
- 529 14. Bond, G. *et al.* Persistent solar influence on north atlantic climate during the Holocene. *Science (80-.)*.
530 **294**, 2130–2136 (2001).
- 531 15. deMenocal, P. *et al.* Abrupt onset and termination of the African Humid Period: *Quat. Sci. Rev.* **19**,
532 347–361 (2000).
- 533 16. Claussen, M., Kubatzki, C., Brovkin, V. & Ganopolski, A. Simulation of an abrupt change in Saharan
534 vegetation in the mid-Holocene. *Geophys. Res. Lett.* **26**, 2037–2040 (1999).
- 535 17. Haug, G. H., Hughen, K. A., Sigman, D. M., Peterson, L. C. & Röhl, U. Southward migration of the
536 intertropical convergence zone through the holocene. *Science (80-.)*. **293**, 1304–1308 (2001).
- 537 18. Kuhlmann, H., Meggers, H., Freudenthal, T. & Wefer, G. The transition of the monsoonal and the N
538 Atlantic climate system off NW Africa during the Holocene. *Geophys. Res. Lett.* **31**, 1–4 (2004).
- 539 19. McGee, D., Donohoe, A., Marshall, J. & Ferreira, D. Changes in ITCZ location and cross-equatorial
540 heat transport at the Last Glacial Maximum, Heinrich Stadial 1, and the mid-Holocene. *Earth Planet.*
541 *Sci. Lett.* **390**, 69–79 (2014).
- 542 20. Kuhlmann, H., Freudenthal, T., Helmke, P. & Meggers, H. Reconstruction of paleoceanography off
543 NW Africa during the last 40,000 years: Influence of local and regional factors on sediment
544 accumulation. *Mar. Geol.* **207**, 209–224 (2004).
- 545 21. Tierney, J. E., Pausata, F. S. R. & DeMenocal, P. B. Rainfall regimes of the Green Sahara. *Sci. Adv.* **3**,
546 (2017).
- 547 22. Jolly, D., Harrison, S. P., Damnati, B. & Bonnefille, R. Simulated climate and biomes of Africa during
548 the late Quaternary: Comparison with pollen and lake status data. *Quat. Sci. Rev.* **17**, 629–657 (1998).
- 549 23. Shanahan, T. M. *et al.* Atlantic forcing of persistent drought in West Africa. *Science (80-.)*. **324**, 377–
550 380 (2009).

- 551 24. Claussen, M., Dallmeyer, A. & Bader, J. *Theory and Modeling of the African Humid Period and the*
552 *Green Sahara*. vol. 1 (Oxford University Press, 2017).
- 553 25. Specht, N. F., Claussen, M. & Kleinen, T. Simulated range of mid-Holocene precipitation changes
554 from extended lakes and wetlands over North Africa. *Clim. Past* **18**, 1035–1046 (2022).
- 555 26. Kröpelin, S. *et al.* Climate-Driven Ecosystem Succession in the Sahara: The Past 6000 Years. *Science*
556 *(80-.)*. **320**, 765–768 (2008).
- 557 27. Blois, C., Forman, S. L. & Wright, D. K. Water level history for Lake Turkana, Kenya in the past
558 15,000 years and a variable transition from the African Humid Period to Holocene aridity. *Glob. Planet.*
559 *Change* **132**, 64–76 (2015).
- 560 28. Höpker, S. N. *et al.* Pronounced Northwest African Monsoon Discharge During the Mid- to Late
561 Holocene. *Front. Earth Sci.* **7**, 1–17 (2019).
- 562 29. Tjallingii, R. *et al.* Coherent high- and low-latitude control of the northwest African hydrological
563 balance. *Nat. Geosci.* **1**, 670–675 (2008).
- 564 30. Armitage, S. J., Bristow, C. S. & Drake, N. A. West African monsoon dynamics inferred from abrupt
565 fluctuations of Lake Mega-Chad. *Proc. Natl. Acad. Sci.* **112**, 8543–8548 (2015).
- 566 31. Faure, H. Changements climatiques au sud des régions méditerranéennes: le Sahara et le Sahel au
567 Quaternaire. in *Quaternary climate in Western Mediterranean* (ed. Lopez-Vera, F.) 533–534
568 (Universidad Autónoma, 1986).
- 569 32. Wengler, L. & Vernet, J. L. Vegetation, sedimentary deposits and climates during the Late Pleistocene
570 and Holocene in eastern Morocco. *Palaeogeogr. Palaeoclimatol. Palaeoecol.* **94**, 141–167 (1992).
- 571 33. Weldeab, S., Lea, D. W., Schneider, R. R. & Andersen, N. 155,000 Years of West African Monsoon
572 and Ocean Thermal Evolution. *Science (80-.)*. **316**, 1303–1307 (2007).
- 573 34. Ghandour, I. M. *et al.* Mid-Late Holocene Paleoenvironmental and Sea Level Reconstruction on the Al
574 Lith Red Sea Coast, Saudi Arabia. *Front. Mar. Sci.* **8**, 1–20 (2021).
- 575 35. Ritchie, J. C., Eyles, C. H. & Haynes, C. V. Sediment and pollen evidence for an early to mid-
576 Holocene humid period in the eastern Sahara. *Nature* **314**, 352–355 (1985).
- 577 36. Sha, L., Brahim, Y. A., Wassenburg, J. A., Yin, J. & Peros, M. How Far North Did the African
578 Monsoon Fringe Expand During the African Humid Period? Insights From Southwest Moroccan

- 579 Speleothems Geophysical Research Letters. 93–102 (2019) doi:10.1029/2019GL084879.
- 580 37. Baqloul, A. *et al.* Climate and land-use effects on hydrological and vegetation signals during the last
581 three millennia: Evidence from sedimentary leaf waxes in southwestern Morocco. *Holocene* **31**, 699–
582 708 (2021).
- 583 38. Raynal, J. & Ballouche, A. Nouvelles données sur la formation des systèmes lagunaires atlantiques
584 marocains pendant le cycle mellahien. (1985) doi:10.13140/RG.2.1.2517.3928.
- 585 39. Ballouche, A. & Carruesco, C. Evolution holocène d'un écosystème lagunaire : la lagune de Oualidia
586 (Maroc atlantique). *Rev. géologie Dyn. géographie Phys.* **27**, 113–118 (1986).
- 587 40. Beaubrun, P.-C., Thevenot, M. & Schouten, J. R. Wintering and summering water bird populations in
588 the Khnifiss Lagoon. in *The Khnifiss lagoon and its surrounding environment (Province of L'ayoune,*
589 *Morocco)* (eds. Dakki, M. & Ligny, W. de) 125–140 (Trav. Inst. Sci., 1988).
- 590 41. Dakki, M. & Ligny, W. de. *The Khnifiss lagoon and its surrounding environment (Province of*
591 *L'ayoune, Morocco)*. *Trav. Inst. Sci.* (1988).
- 592 42. Dakki, M. & Parker, D. M. The Khnifiss Lagoon and adjacent desert area: geographical description
593 and recent coastline changes. in *The Khnifiss lagoon and its surrounding environment (Province of*
594 *L'ayoune, Morocco)* (eds. Dakki, M. & Ligny, W. de) 2–6 (1988).
- 595 43. Idrissi, J. L. *et al.* Organisation et fonctionnement d'un écosystème côtier du Maroc : la lagune de
596 Khnifiss. *Rev. des Sci. l'eau* **17**, 447–462 (2004).
- 597 44. Ait Brahim, Y. *et al.* Speleothem records decadal to multidecadal hydroclimate variations in
598 southwestern Morocco during the last millennium. *Earth Planet. Sci. Lett.* **476**, 1–10 (2017).
- 599 45. Nogueira, J. *et al.* Coastal wetland responses to a century of climate change in northern Sahara,
600 Morocco. *Limnol. Oceanogr.* **67**, 285–299 (2022).
- 601 46. McGregor, H. V, Dima, M., Fischer, H. W. & Mulitza, S. Rapid 20th-Century Increase in Coastal
602 Upwelling off Northwest Africa. *Science (80-.)*. **315**, 637–639 (2007).
- 603 47. Agbani, M. A. El, Fekhaoui, M., Bayed, A. & Schouten, J. R. The Khnifiss Lagoon and adjacent
604 waters: hydrology and hydrodynamics. in *The Khnifiss Lagoon and its surrounding environment*
605 *(Province of La'youne, Morocco)* (eds. Dakki, M. & Ligny, W. de) 17–26 (Trav. Inst. Sci., 1988).
- 606 48. Bond, G. *et al.* Persistent Solar Influence on North Atlantic Climate During the Holocene. *Science (80-*

- 607 .). **294**, 2130–2136 (2001).
- 608 49. Bond, G. *et al.* A pervasive millennial-scale cycle in North Atlantic Holocene and glacial climates.
609 *Science* (80-.). **278**, 1257–1266 (1997).
- 610 50. Cheddadi, R., Lamb, H. F., Guiot, J. & Van Der Kaars, S. Holocene climatic change in Morocco: A
611 quantitative reconstruction from pollen data. *Clim. Dyn.* **14**, 883–890 (1998).
- 612 51. Mook, W. G. & van der Plicht, J. Reporting 14 C Activities and Concentrations. *Radiocarbon* **41**, 227–
613 239 (1999).
- 614 52. Ndiaye, A. *et al.* Reconstruction of the holocene climate and environmental changes of Niayes peat
615 bog in northern coast of Senegal (NW Africa) based on stable isotopes and charcoals analysis. *Quat.*
616 *Sci. Rev.* **289**, 107609 (2022).
- 617 53. PannoZZo, N., Smedley, R. K., Plater, A. J., Carnacina, I. & Leonardi, N. Novel luminescence
618 diagnosis of storm deposition across intertidal environments. *Sci. Total Environ.* **867**, 161461 (2023).
- 619 54. Ballouche, A., Lefevre, D., Carruesco, C., Raynal, J. P. & Texier, J. P. Holocene environments of
620 coastal and continental Morocco. *Quat. Clim. West. Mediterr.* 517–531 (1986)
621 doi:10.13140/2.1.1724.7529.
- 622 55. Winsemann, J., Hartmann, T., Lang, J., Fälber, R. & Lauer, T. Depositional architecture and
623 aggradation rates of sand-rich, supercritical alluvial fans: Control by autogenic processes or high-
624 frequency climatic oscillations? *Sediment. Geol.* **440**, (2022).
- 625 56. Torfstein, A., Gavrieli, I., Katz, A., Kolodny, Y. & Stein, M. Gypsum as a monitor of the paleo-
626 limnological-hydrological conditions in Lake Lisan and the Dead Sea. *Geochim. Cosmochim. Acta* **72**,
627 2491–2509 (2008).
- 628 57. Parker, D., Bell, R. & Pye, S. Soils of the coastal platform between Khnifiss Lagoon and Tarfaya. in
629 *The Khnifiss Lagoon and its surrounding environment (Province of La'youne, Morocco)* (eds.
630 Mohamed Dakki & Ligny, W. De) 172 (Trav. Inst. Sci., 1988).
- 631 58. Martin-Puertas, C. *et al.* Regional atmospheric circulation shifts induced by a grand solar minimum.
632 *Nat. Geosci.* **5**, 397–401 (2012).
- 633 59. Hurrell, J. W. Decadal Trends in the North Atlantic Oscillation: Regional Temperatures and
634 Precipitation. *Science* (80-.). **269**, 676–679 (1995).

- 635 60. Orme, L. C. *et al.* Aeolian sediment reconstructions from the Scottish Outer Hebrides: Late Holocene
636 storminess and the role of the North Atlantic Oscillation. *Quat. Sci. Rev.* **132**, 15–25 (2016).
- 637 61. Goslin, J. *et al.* Holocene centennial to millennial shifts in North-Atlantic storminess and ocean
638 dynamics. *Sci. Rep.* **8**, 1–12 (2018).
- 639 62. Brayshaw, D. J., Hoskins, B. & Black, E. Some physical drivers of changes in the winter storm tracks
640 over the North Atlantic and Mediterranean during the Holocene. *Philos. Trans. R. Soc. A Math. Phys.*
641 *Eng. Sci.* **368**, 5185–5223 (2010).
- 642 63. Bakke, J., Lie, Ø., Dahl, S. O., Nesje, A. & Bjune, A. E. Strength and spatial patterns of the Holocene
643 wintertime westerlies in the NE Atlantic region. *Glob. Planet. Change* **60**, 28–41 (2008).
- 644 64. Orme, L. C. *et al.* Past changes in the North Atlantic storm track driven by insolation and sea-ice
645 forcing. *Geology* **45**, 335–338 (2017).
- 646 65. Bond, G. *et al.* A Pervasive Millennial-Scale Cycle in North Atlantic Holocene and Glacial Climates.
647 *Science (80-.)*. **278**, 1257–1266 (1997).
- 648 66. Zielhofer, C. *et al.* Western Mediterranean hydro-climatic consequences of Holocene ice-rafted debris
649 (Bond) events. *Clim. Past* **15**, 463–475 (2019).
- 650 67. Deaton, C. D., Hein, C. J. & Kirwan, M. L. Barrier island migration dominates ecogeomorphic
651 feedbacks and drives salt marsh loss along the Virginia Atlantic Coast, USA. *Geology* (2017)
652 doi:10.1130/G38459.1.
- 653 68. Schuerch, M. *et al.* Future response of global coastal wetlands to sea-level rise. *Nature* (2018)
654 doi:10.1038/s41586-018-0476-5.
- 655 69. Roman, C. T., Peck, J. A., Allen, J. R., King, J. W. & Appleby, P. G. Accretion of a New England
656 (U.S.A.) salt marsh in response to inlet migration, storms, and sea-level rise. *Estuar. Coast. Shelf Sci.*
657 (1997) doi:10.1006/ecss.1997.0236.
- 658 70. Więski, K., Guo, H., Craft, C. B. & Pennings, S. C. Ecosystem Functions of Tidal Fresh, Brackish, and
659 Salt Marshes on the Georgia Coast. *Estuaries and Coasts* **33**, 161–169 (2010).
- 660 71. FitzGerald, D. M. Shoreline Erosional-Depositional Processes Associated with Tidal Inlets. *Hydrodyn.*
661 *Sediment Dyn. Tidal Inlets* **29**, 186–225 (1988).
- 662 72. Khalfaoui, O. *et al.* Paleoenvironmental evolution and evidence of marine submersion events from

- 663 mid-to late Holocene in northwestern Morocco: The case of the Tahaddart lower estuary. *Cont. Shelf*
664 *Res.* **256**, 104958 (2023).
- 665 73. Weisrock, A. L. E. Late-middle pleistocene, late pleistocene and holocene palaeo-sea-level records at
666 agadir and the atlantic atlas coastal reach, morocco: An updated overview. *Quaternaire* **23**, 211–225
667 (2012).
- 668 74. Petit-Maire, N. Holocene biogeographical variation along the northwestern African coast (28 - 19 N).
669 in *Sahara and the surrounding areas* (eds. Sarnthein, M., Seibold, E. & Rognon, P.) 365–377
670 (Balkema, 1980).
- 671 75. Zazo, C. *et al.* The coastal archives of the last 15ka in the Atlantic–Mediterranean Spanish linkage
672 area: Sea level and climate changes. *Quat. Int.* **181**, 72–87 (2008).
- 673 76. Lario, J. *et al.* Holocene palaeotsunami catalogue of SW Iberia. *Quat. Int.* **242**, 196–200 (2011).
- 674 77. Ruiz, F. *et al.* Geomorphology Sedimentological and geomorphological imprints of Holocene tsunamis
675 in southwestern Spain : An approach to establish the recurrence period. *Geomorphology* **203**, 97–104
676 (2013).
- 677 78. Jalut, G., Esteban Amat, A., Bonnet, L., Gauquelin, T. & Fontugne, M. Holocene climatic changes in
678 the Western Mediterranean, from south-east France to south-east Spain. *Palaeogeogr. Palaeoclimatol.*
679 *Palaeoecol.* **160**, 255–290 (2000).
- 680 79. Santos, L., Sánchez-Goñi, M. F., Freitas, M. C. & Andrade, C. Climatic and environmental changes in
681 the Santo André coastal area (SW Portugal) during the last 15,000 years. in *Quaternary climatic*
682 *changes and environmental crises in the Mediterranean Region* 175–179 (2003).
- 683 80. Zielhofer, C., Bussmann, J., Ibouhouten, H. & Fenech, K. Flood frequencies reveal Holocene rapid
684 climate changes (Lower Moulouya River, northeastern Morocco). *J. Quat. Sci.* **25**, 700–714 (2010).
- 685 81. Olsen, J., Anderson, N. J. & Knudsen, M. F. Variability of the North Atlantic Oscillation over the past
686 5,200 years. *Nat. Geosci.* **5**, 808–812 (2012).
- 687 82. Holz, C., Stuut, J. B. W., Henrich, R. & Meggers, H. Variability in terrigenous sedimentation processes
688 off northwest Africa and its relation to climate changes: Inferences from grain-size distributions of a
689 Holocene marine sediment record. *Sediment. Geol.* **202**, 499–508 (2007).
- 690 83. Kim, J. H. *et al.* Impacts of the North Atlantic gyre circulation on Holocene climate off northwest

- 691 Africa. *Geology* **35**, 387–390 (2007).
- 692 84. Bouimetarhan, I. *et al.* Palynological evidence for climatic and oceanic variability off NW Africa
693 during the late Holocene. *Quat. Res.* **72**, 188–197 (2009).
- 694 85. Woodruff, J. D., Irish, J. L. & Camargo, S. J. Coastal flooding by tropical cyclones and sea-level rise.
695 *Nature* **504**, 44–52 (2013).
- 696 86. Dezileau, L. *et al.* Intense storm activity during the Little Ice Age on the French Mediterranean coast.
697 *Palaeogeogr. Palaeoclimatol. Palaeoecol.* **299**, 289–297 (2011).
- 698 87. Cheddadi, R., Lamb, H. F., Guiot, J. & Van Der Kaars, S. Holocene climatic change in Morocco: A
699 quantitative reconstruction from pollen data. *Clim. Dyn.* **14**, 883–890 (1998).
- 700 88. Knippertz, P., Christoph, M. & Speth, P. Long-term precipitation variability in Morocco and the link to
701 the large-scale circulation in recent and future climates. *Meteorol. Atmos. Phys.* **83**, 67–88 (2003).
- 702 89. Jalali, B., Sicre, M.-A., Azuara, J., Pellichero, V. & Combourieu-Nebout, N. Influence of the North
703 Atlantic subpolar gyre circulation on the 4.2 ka BP event. *Clim. Past* **15**, 701–711 (2019).
- 704 90. McGee, D., deMenocal, P. B., Winckler, G., Stuut, J. B. W. & Bradtmiller, L. I. The magnitude, timing
705 and abruptness of changes in North African dust deposition over the last 20,000 yr. *Earth Planet. Sci.*
706 *Lett.* **371–372**, 163–176 (2013).
- 707 91. Collins, J. A. *et al.* Rapid termination of the African Humid Period triggered by northern high-latitude
708 cooling. *Nat. Commun.* **8**, 1372 (2017).
- 709 92. Roberts, N. *The Holocene: an environmental history.* (John Wiley & Sons, 2014).
- 710 93. Weisrock, A. *Geomorphologie et Paléoenvironnements de l'Atlas atlantique, Maroc.* (Notes et Memoires
711 du Service Geologique du Maroc, 1993).
- 712 94. Weisrock, A. *Geomorphologie et paléoenvironnements de l'Atlas atlantique, Maroc.* (Universite Paris I
713 Pantheon-Sorbonne, 1980).

714

715